Neutrino mass ordering: Circumventing the challenges using synergy between T2HK and JUNO

Sandhya Choubey*

Department of Physics, School of Engineering Sciences, KTH Royal Institute of Technology, AlbaNova University Center, Roslagstullsbacken 21, SE–106 91 Stockholm, Sweden and The Oskar Klein Centre for Cosmoparticle Physics, AlbaNova University Center, Roslagstullsbacken 21, SE–106 91 Stockholm, Sweden

Monojit Ghosh†

School of Physics, University of Hyderabad, Hyderabad—500046, India and Center of Excellence for Advanced Materials and Sensing Devices, Ruder Bošković Institute, 10000 Zagreb, Croatia

Deepak Raikwal‡

Harish-Chandra Research Institute, A CI of Homi Bhabha National Institute, Chhatnag Road, Jhunsi, Prayagraj 211019, India and Homi Bhabha National Institute, Anushakti Nagar, Mumbai 400094, India

(Received 18 July 2022; accepted 17 November 2022; published 13 December 2022)

One of the major open problems of neutrino physics is mass ordering (MO). We discuss the prospects of measuring MO with two under-construction experiments T2HK and JUNO. JUNO alone is expected to measure MO with greater than 3σ significance as long as certain experimental challenges are met. In particular, JUNO needs better than 3% energy resolution for MO measurement. On the other hand, T2HK has rather poor prospects at measuring the MO, especially for certain ranges of the CP violating parameter δ_{CP}, posing a major drawback for T2HK. In this article we show that the synergy between JUNO and T2HK will bring twofold advantage. First, the synergy between the two experiments helps us determine the MO at a very high significance. With the baseline setup of the two experiments, we have a greater than 9σ determination of the MO for all values of δ_{CP}. Second, the synergy also allows us to relax the constraints on the two experiments. We show that JUNO could perform extremely well even for an energy resolution of 5%, while for T2HK the MO problem with "bad" values of δ_{CP} goes away. The MO sensitivity for the combined analysis is expected to be greater than 6σ for all values of δ_{CP} and with just 5% energy resolution for JUNO.

DOI: 10.1103/PhysRevD.106.115013

I. INTRODUCTION

Despite the big strides made in the field of neutrino physics, we still lack knowledge of some of the important neutrino parameters. The neutrino mass ordering (MO) is a prime example and measuring it will have far-reaching consequences both theoretically as well as experimentally. By MO we essentially mean the structure of the neutrino mass spectrum. For three generations of neutrinos, one can define two mass-squared differences, which we call Δm^2_{21} and Δm^2_{31} ($\Delta m^2_{ij} = m^2_i - m^2_j$). While it is experimentally known that $\Delta m^2_{21} > 0$, the sign of Δm^2_{31} is still not statistically confirmed. The case with $\Delta m^2_{31} > 0$ is referred to as the normal mass ordering (NO), while $\Delta m^2_{31} < 0$ is called inverted mass ordering (IO) [1].

Experiments are being built that would be able to shed light on MO. Such experiments are expensive as well as challenging. The JUNO experiment [2] is being built in China specifically to determine the MO [3–6]. JUNO would observe electron antineutrinos from powerful Chinese reactors and must reach an energy resolution of at least 3% or better in order to achieve a modest statistical significance. This is a major technological challenge and so-far unprecedented. On the other hand, the T2HK experiment [7] under construction will be observing muon- and electron-type neutrinos (and antineutrinos) from accelerator

*choubey@kth.se
†monojit_rfp@uohyd.ac.in
‡deepakraikwal@hri.res.in

facilities in Japan [8–22]. This experiment has measurement of the CP violating phase δ_{CP} as its major goal. However, the unresolved MO is a major challenge for this experiment that leads to a deterioration of its sensitivity. In fact, T2HK's MO sensitivity is rather low, particularly for $\delta_{CP} = 0°$. In this article we will study the synergy between these two experiments and show for the first time that combining the data from just these two experiments will (i) determine MO to very high significance and (ii) reduce the challenges they face. In particular, we will show that JUNO would be able to perform remarkably well for energy resolutions of even 5%, for which even the current technology suffices. This will bring down both the technological demand as well as costs on JUNO.

In this article we will focus on the role of $|\Delta m^2_{31}|$ in the MO determination. Data corresponding to NO can be mimicked (or fitted) by a theory corresponding to IO by changing the value of $|\Delta m^2_{31}|$ in the fit. We will show, both analytically as well as numerically, how different neutrino oscillation channels change $|\Delta m^2_{31}|$ differently in the fit. This change is also dependent on the neutrino energy; therefore, different neutrino energy bins would require different amounts of shift in $|\Delta m^2_{31}|$. Since the experiments depend on different oscillation channels and since we also have spectral information in these experiments, this leads to a spectacular synergy between different experiments, as well as between different data bins of the same experiment.

In another study [23] we will include the future atmospheric neutrino experiment ICAL at the INO facility [24] and will be focusing on how its sensitivity is affected due to synergy with JUNO and T2HK. However, the main focus of the present work is twofold. First, we study quantitatively how much the synergy between JUNO and T2HK improves the MO sensitivity of the combined setup. Second, and even more importantly, we study how the synergy helps in reducing the energy resolution requirement on JUNO. We will quantitatively show that, even if JUNO is unable to reach its design energy resolution of 3%, we would still be able to measure the MO with high significance. Therefore, the two papers are complementary to each other.

II. THE METHOD

The expected MO sensitivity for these future facilities is estimated by the following method. The prospective data are calculated for these experiments assuming NO. This simulated data are then statistically fitted with a theory of IO by defining a χ^2. We simulate both T2HK and JUNO using the GLoBES software [25,26]. For details of the experimental parameters used in this work, we refer the reader to [7] for T2HK and [2] for JUNO. For T2HK we have two kinds of datasets. The data on muon (and antimuon) events depend on the $\nu_\mu \to \nu_\mu$ survival probability $P_{\mu\mu}$, which is referred to as the "disappearance channel." On the other hand, the data on electron (and positron) events depend on the $\nu_\mu \to \nu_e$ conversion probability $P_{\mu e}$ and is referred to as the "appearance channel." JUNO has only a dataset for positrons, which depends on the $\bar{\nu}_e \to \bar{\nu}_e$ survival probability $P_{\bar{e}\bar{e}}$.

TABLE I. The best-fit values and 3σ ranges of the oscillation parameters used in our calculation.

Parameter	Best-fit value	3σ range
θ_{12}	33.44°	...
θ_{13}	8.57°	...
θ_{23}	45°	40° to 52°
δ_{CP}	−90°/0°	−180° to 180°
Δm^2_{21}	7.42×10^{-5} eV^2	...
Δm^2_{31}	2.531×10^{-3} eV^2	(2.435 to 2.598) $\times 10^{-3}$ eV^2

The "data" for T2HK and JUNO are simulated for NO at the values of the oscillation parameters given in column 2 of Table I. We fit the data with IO and allow θ_{23}, δ_{CP}, and $|\Delta m^2_{31}|$ to vary in the range given in column 3 of Table I. The parameters θ_{12}, θ_{13}, and Δm^2_{21} are kept fixed in the fit at their values given in column 2.

III. THE PIVOTAL ROLE OF $|\Delta m^2_{31}|$

For both T2HK and JUNO, matter effects are negligible and the survival probability of ν_α, where $\alpha = e$ or μ, can be approximately given as

$$P_{\alpha\alpha} = 1 - 4|U_{\alpha 1}|^2|U_{\alpha 2}|^2\sin^2\Delta_{21} - 4|U_{\alpha 1}|^2|U_{\alpha 3}|^2\sin^2\Delta_{31} - 4|U_{\alpha 2}|^2|U_{\alpha 3}|^2\sin^2\Delta_{32}, \quad (1)$$

where $\Delta_{ij} = \Delta m^2_{ij}L/4E$, L being the distance that the neutrino travels and E its energy. This gives $P^{\rm NO}_{\alpha\alpha}$ for $\Delta^{\rm NO}_{31}$ and $P^{\rm IO}_{\alpha\alpha}$ for $\Delta^{\rm IO}_{31}$ and one can obtain an analytic expression for $\Delta P_{\alpha\alpha} = P^{\rm NO}_{\alpha\alpha} - P^{\rm IO}_{\alpha\alpha}$. Note that since $\Delta m^2_{32} = \Delta m^2_{31} - \Delta m^2_{21}$, and since we keep $\Delta m^2_{21} > 0$ fixed, we have

$$\Delta P_{\alpha\alpha} = -4|U_{\alpha 3}|^2[|U_{\alpha 1}|^2(\sin^2\Delta^{\rm NO}_{31} - \sin^2\Delta^{\rm IO}_{31}) - |U_{\alpha 2}|^2(\sin^2(\Delta^{\rm NO}_{31} - \Delta_{21}) - \sin^2(\Delta^{\rm IO}_{31} + \Delta_{21}))], \quad (2)$$

Equation (2) shows that $\Delta P_{\alpha\alpha}$ cannot be zero for $|\Delta^{\rm NO}_{31}| = |\Delta^{\rm IO}_{31}|$ since the second term becomes nonzero for this case. This term will reduce in magnitude if $|\Delta^{\rm IO}_{31}|$ is reduced, however, then the first term becomes nonzero. Note that the first term is weighted by $|U_{\alpha 1}|^2$, while the second term is weighted by $|U_{\alpha 2}|^2$. Therefore, the minimum of $\Delta P_{\alpha\alpha}$ comes at a value of $|\Delta^{\rm IO}_{31}|$ that is lower than $|\Delta^{\rm NO}_{31}|$ roughly by Δm^2_{21} weighted by a factor that depends on $|U_{\alpha 1}|^2$ and $|U_{\alpha 2}|^2$. Therefore, the following points are evident. Since the mass ordering sensitivity is given in terms $\Delta P_{\alpha\alpha}$, if the data correspond to NO, then the fit will change the value of $|\Delta^{\rm IO}_{31}|$ such that $\Delta P_{\alpha\alpha}$ is minimized. Also, if

$\Delta_{31}^{\rm IO} = -\Delta_{31}^{\rm NO} + x$, then x will be different for P_{ee} and $P_{\mu\mu}$ since it depends on $|U_{\alpha 1}|^2$ and $|U_{\alpha 2}|^2$. Therefore, (1) the best-fit value of Δm_{31}^2 is different for T2HK and JUNO leading to synergy between them. Also, since the discussion above involves $\Delta_{31} = \Delta m_{31}^2 L/4E$, the minima of $\Delta P_{\alpha\alpha}$ will appear at different values of Δm_{31}^2 (IO) for different values of E; (2) even within the same experiment, the different E bins will have a different best-fit Δm_{31}^2 (IO), leading to synergy even within the same experiment. Finally, (3) T2HK also has the appearance channel $P_{\mu e}$ which gives best-fit Δm_{31}^2 (IO) at a different value leading to further synergy. We will show how the synergy between $P_{\mu\mu}$ and $P_{\mu e}$ also leads to increase in MO sensitivity of T2HK. We show how the three above-mentioned synergies lead to an increase of MO sensitivity.

A. T2HK

For the disappearance channel, following the discussion above, we note that close to the Δm_{31}^2 oscillation maximum, the minima for $\Delta P_{\mu\mu}$ appears when [27,28]

$$x = \frac{2|U_{\mu 2}|^2}{|U_{\mu 1}|^2 + |U_{\mu 2}|^2} \Delta m_{21}^2. \tag{3}$$

For our choice of oscillation parameters, we obtain $x = 0.0813 \times 10^{-3}$ eV^2, giving $\Delta m_{31}^2(\text{IO}) = (-2.531 + 0.0813) \times 10^{-3}$ eV$^2 = -2.4497 \times 10^{-3}$ eV^2. We show $\Delta P_{\mu\mu}$ in Fig. 1 for $L = 295$ km and two neutrino energies $E = 0.6$ and 0.7 GeV. This figure has been obtained from a numerical calculation of the full three-generation oscillation probability including Earth matter effects.

Note that, for the disappearance channel, NO can be matched almost exactly by IO for $\Delta m_{31}^2(\text{IO}) \approx -2.4497 \times 10^{-3}$ eV^2, which agrees well with Eq. (3). Note that we get $\Delta P_{\mu\mu} \simeq 0$ at almost the same value of Δm_{31}^2 (IO) for both energies since they are both close to the oscillation maxima. The figure also shows the appearance channel. Since the appearance channel has more matter effects, $\Delta P_{\mu e}$ is never zero and the best-fit Δm_{31}^2 (IO) comes at a different value.

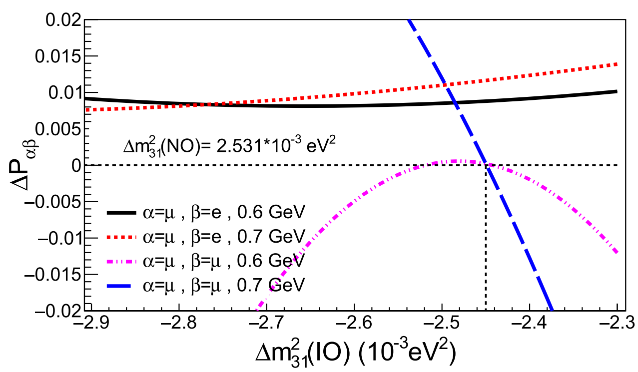

FIG. 1. $\Delta P_{\mu\mu}$ and $\Delta P_{\mu e}$ as a function of Δm_{31}^2 (IO) for $L = 295$ km and two values of energy.

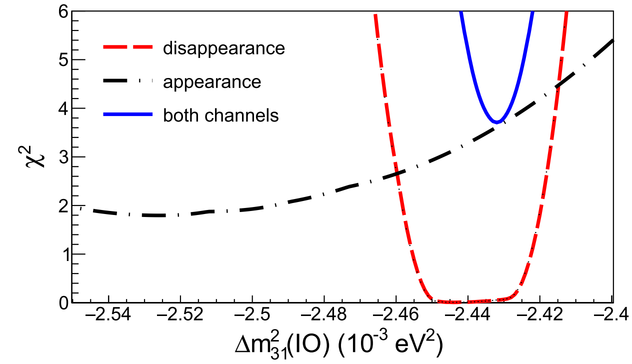

FIG. 2. Mass ordering sensitivity χ^2 as a function of Δm_{31}^2 (IO) for T2HK.

In Fig. 2 we show the effect of combining the disappearance and the appearance channels in T2HK in a χ^2 plot. One can see that the minima in Δm_{31}^2 (IO) for the disappearance channel comes very close to that predicted in Eq. (3) and Fig. 1 and different as compared to the assumed true value. For the appearance channel, the Δm_{31}^2 (IO) dependence of the χ^2 is shallow in comparison; nevertheless, it too has a distinct minimum, which is not only different from the assumed true value, but also different with the minimum for the disappearance channel. As a result, when we combine them (blue line) we get a significantly higher χ^2.

B. JUNO

The Eqs. (1) and (2) are also valid for JUNO and studies on JUNO along these lines have been performed before [29]. Here we propose a somewhat novel approach. Note that Eq. (2) is given in terms of $\Delta_{31}^{\rm IO}$ which depends on both Δm_{31}^2 (IO) and E. Since T2HK is a narrow band beam peaked at its oscillation maximum, it was enough to work at E corresponding to oscillation maximum. However, JUNO is a wide band beam and E plays an important role here. This essentially means that for each E we will have a different value of Δm_{31}^2 (IO) that will give $\Delta P_{\bar{e}\bar{e}} = 0$. So we compute analytically and find solutions for

$$\frac{\partial(\Delta P_{\bar{e}\bar{e}})}{\partial \Delta_{31}^{\rm IO}} = 0, \tag{4}$$

giving us the following relation:

$$\cos^2\theta_{12} \sin 2\Delta_{31}^{\rm IO} + \sin^2\theta_{12} \sin 2(\Delta_{31}^{\rm IO} - \Delta_{21}) - \cos^2\theta_{12} \sin 2\Delta_{31}^{\rm NO} . \frac{\Delta_{31}^{\rm NO}}{\Delta_{31}^{\rm IO}} - \sin^2\theta_{12} \sin 2\Delta_{32}^{\rm NO} \frac{\Delta_{32}^{\rm NO}}{\Delta_{31}^{\rm IO}} = 0.$$

This is a relation between E and Δm_{31}^2 (IO) that gives us a minimum in $\Delta P_{\bar{e}\bar{e}}$. The reactor antineutrino event spectrum that we consider for JUNO varies between $E = 1.8$ and 8 MeV and is divided into 200 equispaced bins,

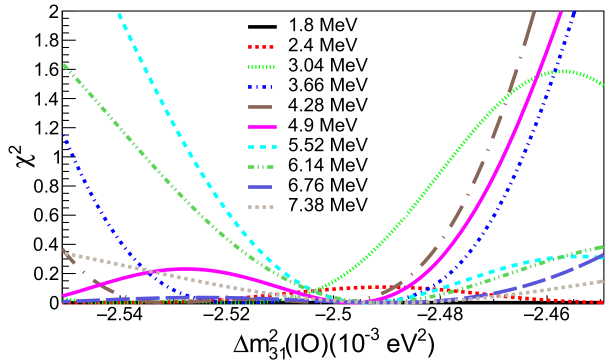

FIG. 3. Mass ordering χ^2 in JUNO for 10 energy bins out of the total 200 energy bins. Systematic uncertainties are neglected.

TABLE II. Values of Δm^2_{31} (IO) (in units of 10^{-3} eV^2), for which we get mass ordering χ^2 minimum.

	JUNO	T2HK	JUNO + T2HK	True value
$\delta_{CP} = 0°$	−2.503	−2.432	−2.481	2.531
$\delta_{CP} = -90°$	−2.503	−2.429	−2.479	2.531

TABLE III. Mass ordering χ^2 for true NO and test IO. We label the χ^2 for JUNO and T2HK as χ^2_J and χ^2_T, respectively.

NO	χ^2_J	χ^2_T	$\chi^2_J + \chi^2_T$	χ^2_{J+T}	% increase
$\delta_{CP} = 0°$	10.23	3.70	13.93	86.87	523
$\delta_{CP} = -90°$	10.23	25.07	35.30	113.22	220

with a bin width of 0.031 MeV. For the sake of illustration, we compute the mass ordering χ^2 for each bin in JUNO, neglecting all systematic uncertainties and show these for ten example bins in Fig. 3. We note two important points from this figure. First, the different E bins give χ^2 minimum at different values of Δm^2_{31} (IO). Second, and even more importantly, note that $\chi^2_{\rm min} \simeq 0$ in each of the individual bins, albeit at a different value of Δm^2_{31} (IO). Hence, when we do the combined analysis of all 200 bins, we get $\chi^2 = 10$. This is due to the synergy between the different E bins of JUNO as described above. The best-fit Δm^2_{31} (IO) obtained from the full 200 bin analysis of JUNO is different from the assumed true value of Δm^2_{31} (NO) used in the simulated data.

IV. COMBINED SENSITIVITY OF JUNO AND T2HK

Finally, we do a joint analysis of JUNO and T2HK and present our results in Fig. 4. Results are shown in two panels for two cases of $\delta_{CP} = 0°$ and $-90°$ motivated by the recent best-fit values of this parameter by NOνA [30] and T2K [31], respectively. Note that JUNO is independent of both θ_{23} as well as δ_{CP}.

We summarize in Tables II and III the main results of this analysis. The values of Δm^2_{31} (IO) for which we get the minimum χ^2 for JUNO and T2HK individually, as well as for the JUNO and T2HK combined analysis, are given in Table II. In Fig. 4, we show the MO sensitivity as a function of Δm^2_{31} (IO). This figure shows the sensitivity of each oscillation channel in JUNO and T2HK to MO, as well as the synergy between them. We can see from Fig. 4 and Table II that, even though data in both experiments were simulated at the same assumed true value of Δm^2_{31} (NO), the best-fit values of Δm^2_{31} (IO) come out to be different for JUNO and T2HK. As a result, when we perform a combined analysis of the two datasets, the expected MO sensitivity is significantly enhanced. While a simple sum of the χ^2 for JUNO and T2HK gives 13.93 (35.3) for $\delta_{CP} = 0°$ ($-90°$), the combined analysis gives χ^2 of 86.87 (113.22). This is a staggering synergistic increase in the sensitivity, shown in the last column of Table III. In particular, for true $\delta_{CP} = 0°$, T2HK by itself is expected to not even return a $\chi^2_T = 4$ for mass ordering [7]. A simple sum of the χ^2s of T2HK and JUNO (χ^2_J) would still not achieve $\chi^2 = 16$ sensitivity. However, a combined analysis of JUNO and T2HK gives $\chi^2_{J+T} \simeq 87$, which shows a whopping improvement of 523%. For the $\delta_{CP} = -90°$ case, both T2HK and

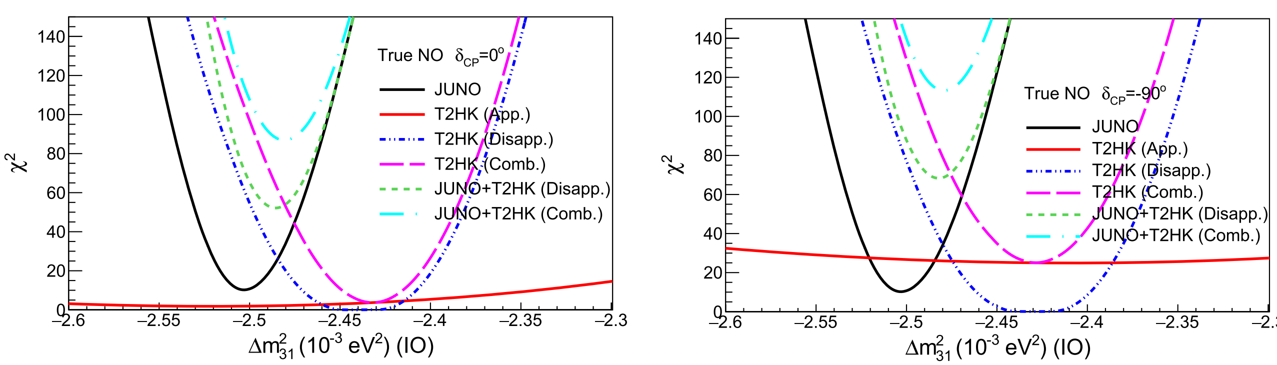

FIG. 4. Mass ordering sensitivity expected from a combined analysis of JUNO and T2HK, shown as a function of Δm^2_{31} (IO). Left: $\delta_{CP} = 0°$. Right: $\delta_{CP} = -90°$.

JUNO individually give a good sensitivity to mass ordering; however, even in this case, doing a combined analysis would lead to mass ordering being discovered with a much higher sensitivity. Let us mention that, for T2HK, the mass ordering sensitivity is very poor for $\delta_{CP} = 0°$ as compared to $\delta_{CP} = -90°$ in normal ordering because of the hierarchy-δ_{CP} degeneracy [32–34]. Indeed for a large fraction of δ_{CP} values, the MO χ^2 for T2HK is below 4. We see from our results above that combining the JUNO data with T2HK's can alleviate this problem and we expect greater than 9σ MO sensitivity for all values of δ_{CP}.

For the sake of understanding the underlying physics, we also show the MO sensitivity of the appearance and the disappearance channels in T2HK separately in Fig. 4. We can see that, while the appearance channel alone has MO sensitivity, its Δm^2_{31} dependence is very shallow. On the other hand, the disappearance channel alone does not have any MO sensitivity, however, it has a very sharp dependence on Δm^2_{31}. As a result, the combined χ^2 to MO from JUNO and the disappearance channel alone of T2HK has a very strong synergy coming from their strong Δm^2_{31} dependence. This can been seen in the green dashed curve of Fig. 4. Addition of the appearance channel improves the sensitivity further, giving the highest possible sensitivity coming from the combination of these two experiments.

It is pertinent to compare the MO sensitivity of the combined JUNO and T2HK setup with the sensitivity of some of the most promising forthcoming experiments, such as DUNE [35], KM3NeT-ORCA [36], and PINGU [37]. The future accelerator-based experiment DUNE can measure MO with at least 10σ (16σ) C.L., for $\delta_{CP} = 0°$ ($-90°$) in its seven years of running irrespective of the true values of θ_{23}. On the other hand, the analysis with the atmospheric neutrinos at the KM3NeT facility can provide a measurement of MO at 4σ after five years of running for $\delta_{CP} = 0°$ and $\theta_{23} = 42°$. For PINGU, which is a proposed low-energy extension to the IceCube experiment, can measure MO by studying the atmospheric neutrinos with a significance of at least 3σ for $\theta_{23} = 45°$ when a 68% uncertainty on the other oscillation parameters are considered in its four years of running. From the above discussion, we understand that the combination of T2HK and JUNO outperforms KM3NeT-ORCA and PINGU. Regarding DUNE, the sensitivity of T2HK + JUNO is comparable to DUNE for $\delta_{CP} = 0°$, but DUNE outperforms T2HK + JUNO for $\delta_{CP} = -90°$.

V. REMEDYING THE ENERGY RESOLUTION CHALLENGE FOR JUNO

In order to achieve 3σ sensitivity for MO, the JUNO detector will need better than 3% energy resolution. This is unprecedented and challenging, as well as expensive. JUNO sensitivity to MO falls sharply with worsening of the energy resolution and is expected to go to below 1σ for 5% energy resolution. Adding T2HK and JUNO and doing a combined analysis can circumvent this challenge. We show in Fig. 5 the $\sqrt{\chi^2}$ of the combined analysis of T2HK and JUNO as a function of the energy resolution in JUNO. We show the results for both $\delta_{CP} = 0°$ and $-90°$. We can see that, even with 5% energy resolution in JUNO, we hope to get MO sensitivity that is well above 6σ for $\delta_{CP} = 0°$. This would further increase to 8σ if $\delta_{CP} = -90°$.

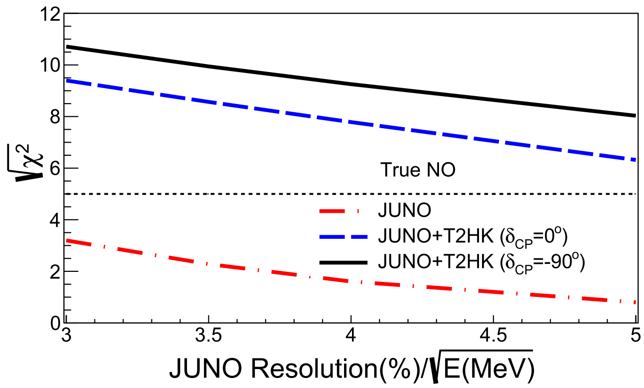

FIG. 5. Expected MO sensitivity $\sqrt{\chi^2}$ as a function of energy resolution of JUNO.

VI. CONCLUSION

Measuring the MO is one of the most important aspects of neutrino physics. Ideally, we want at least 5σ sensitivity to confirm the correct MO. The JUNO experiment is being built to determine the MO; however, it is expected that even to achieve about 3–4σ sensitivity one would need better than 3% energy resolution in JUNO. On the other hand, T2HK being built for *CP* studies has a rather poor MO sensitivity for a large range of δ_{CP} values. This compromises its *CP* sensitivity. In this article, we have shown that there is synergy between these two experiments due to the difference in which their oscillation probabilities depend on $|\Delta m^2_{31}|$. This synergy results in a staggering increase of the expected MO sensitivity when we perform a joint analysis. We showed that this increase could be between 220% and 520% depending on the true value of δ_{CP}. We also showed how this synergy can be instrumental in alleviating the energy resolution challenge for JUNO. We showed that, even with 5% energy resolution in JUNO, the combined analysis gives an expected MO sensitivity of greater than 6σ.

To summarize, we have shown that, due to synergy coming from the $|\Delta m^2_{31}|$ dependence, MO sensitivity of greater than 9σ can be achieved by the combined analysis of JUNO and T2HK. It would be interesting to see if JUNO can achieve 3% energy resolution. We have shown that even if JUNO fails to achieve that, we could still get better than 6σ MO sensitivity from a joint analysis of JUNO with T2HK. Hence, the energy resolution challenge for JUNO is not even needed and the experiment can go ahead with a detector of 5% energy resolution.

ACKNOWLEDGMENTS

The authors would like to thank Suprabh Prakash for providing the .glb file for JUNO and useful discussions regarding the JUNO experiment. M. G. acknowledges the Ramanujan Fellowship of SERB, Government of India, through Grant No. RJF/2020/000082. This project has received funding/support from the European Union's Horizon 2020 research and innovation program under the Marie Skłodowska-Curie Grant Agreement No. 860881-HIDDeN.

[1] I. Esteban, M. C. Gonzalez-Garcia, M. Maltoni, T. Schwetz, and A. Zhou, J. High Energy Phys. 09 (2020) 178.
[2] F. An *et al.* (JUNO Collaboration), J. Phys. G **43**, 030401 (2016).
[3] M. G. Aartsen *et al.* (IceCube-Gen2 Collaboration and JUNO Collaboration Members), Phys. Rev. D **101**, 032006 (2020).
[4] S. Cao, A. Nath, T. V. Ngoc, P. T. Quyen, N. T. Hong Van, and N. K. Francis, Phys. Rev. D **103**, 112010 (2021).
[5] S. Aiello *et al.* (KM3NeT, JUNO Collaborations), J. High Energy Phys. 03 (2022) 055.
[6] D. V. Forero, S. J. Parke, C. A. Ternes, and R. Z. Funchal, Phys. Rev. D **104**, 113004 (2021).
[7] K. Abe *et al.* (Hyper-Kamiokande Collaboration), Prog. Theor. Exp. Phys. **2018**, 063C01 (2018).
[8] M. Ghosh and O. Yasuda, Phys. Rev. D **96**, 013001 (2017).
[9] S. K. Raut, Phys. Rev. D **96**, 075029 (2017).
[10] M. Cho, Y. ChoeJo, H.-S. Lee, Y.-M. Lee, and S. K. Raut, arXiv:1907.01185.
[11] S. K. Agarwalla, M. Ghosh, and S. K. Raut, J. High Energy Phys. 05 (2017) 115.
[12] S. Fukasawa, M. Ghosh, and O. Yasuda, Nucl. Phys. **B918**, 337 (2017).
[13] S. S. Chatterjee, P. Pasquini, and J. W. F. Valle, Phys. Lett. B **771**, 524 (2017).
[14] M. Blennow, P. Coloma, and E. Fernandez-Martinez, J. High Energy Phys. 03 (2015) 005.
[15] S. F. King, S. Molina Sedgwick, S. J. Parke, and N. W. Prouse, Phys. Rev. D **101**, 076019 (2020).
[16] K. Chakraborty, K. N. Deepthi, and S. Goswami, Nucl. Phys. **B937**, 303 (2018).
[17] C. Soumya, K. N. Deepthi, and R. Mohanta, Adv. High Energy Phys. **2016**, 9139402 (2016).
[18] M. Ghosh and T. Ohlsson, Mod. Phys. Lett. A **35**, 2050058 (2020).
[19] P. Coloma, A. Donini, E. Fernandez-Martinez, and P. Hernandez, J. High Energy Phys. 06 (2012) 073.
[20] P. Ballett, S. F. King, S. Pascoli, N. W. Prouse, and T. Wang, Phys. Rev. D **96**, 033003 (2017).
[21] J. Evslin, S.-F. Ge, and K. Hagiwara, J. High Energy Phys. 02 (2016) 137.
[22] P. Panda, M. Ghosh, P. Mishra, and R. Mohanta, Phys. Rev. D **106**, 073006 (2022).
[23] D. Raikwal, S. Choubey, and M. Ghosh, arXiv:2207.06798.
[24] S. Ahmed *et al.* (ICAL Collaboration), Pramana **88**, 79 (2017).
[25] P. Huber, M. Lindner, and W. Winter, Comput. Phys. Commun. **167**, 195 (2005).
[26] P. Huber, J. Kopp, M. Lindner, M. Rolinec, and W. Winter, Comput. Phys. Commun. **177**, 432 (2007).
[27] H. Nunokawa, S. J. Parke, and R. Zukanovich Funchal, Phys. Rev. D **72**, 013009 (2005).
[28] S. K. Raut, Mod. Phys. Lett. A **28**, 1350093 (2013).
[29] L. Stanco, G. Salamanna, F. Sawy, and C. Sirignano, arXiv:1707.07651.
[30] J. Hartnell, *Proceedings of the Neutrino 2022* (Seoul, South Korea, 2022).
[31] C. Bronner, *Proceedings of the Neutrino 2022* (Seoul, South Korea, 2022).
[32] V. Barger, D. Marfatia, and K. Whisnant, Phys. Rev. D **65**, 073023 (2002).
[33] M. Ghosh, P. Ghoshal, S. Goswami, N. Nath, and S. K. Raut, Phys. Rev. D **93**, 013013 (2016).
[34] S. Prakash, S. K. Raut, and S. U. Sankar, Phys. Rev. D **86**, 033012 (2012).
[35] B. Abi *et al.* (DUNE Collaboration), Eur. Phys. J. C **80**, 978 (2020).
[36] S. Adrian-Martinez *et al.* (KM3Net Collaboration), J. Phys. G **43**, 084001 (2016).
[37] M. G. Aartsen *et al.* (IceCube Collaboration), J. Phys. G **44**, 054006 (2017).